

**UNCLASSIFIED**

**A  
D 151286**

**Armed Services Technical Information Agency**

**ARLINGTON HALL STATION  
ARLINGTON 12 VIRGINIA**

**FOR  
MICRO-CARD  
CONTROL ONLY**

**1 OF 1**

**NOTICE: WHEN GOVERNMENT OR OTHER DRAWINGS, SPECIFICATIONS OR OTHER DATA ARE USED FOR ANY PURPOSE OTHER THAN IN CONNECTION WITH A DEFINITELY RELATED GOVERNMENT PROCUREMENT OPERATION, THE U. S. GOVERNMENT THEREBY INCURS NO RESPONSIBILITY, NOR ANY OBLIGATION WHATSOEVER; AND THE FACT THAT THE GOVERNMENT MAY HAVE FORMULATED, FURNISHED, OR IN ANY WAY SUPPLIED THE SAID DRAWINGS, SPECIFICATIONS, OR OTHER DATA IS NOT TO BE REGARDED BY IMPLICATION OR OTHERWISE AS IN ANY MANNER LICENSING THE HOLDER OR ANY OTHER PERSON OR CORPORATION, OR CONVEYING ANY RIGHTS OR PERMISSION TO MANUFACTURE, USE OR SELL ANY PATENTED INVENTION THAT MAY IN ANY WAY BE RELATED THERETO.**

**UNCLASSIFIED**

151286

ASTIA FILE COPY

AD-AS

PROGRESS REPORT NO. 26-2

**CORROSION AND IGNITION OF TITANIUM ALLOYS  
IN FUMING NITRIC ACID**

**II. STUDY OF ADDITIONAL CHEMICAL AND  
METALLURGICAL FACTORS**

JOHN B. RITTENHOUSE

STEPHEN P. VANGO

JULIA S. WHITTICK

**FC**

JET PROPULSION LABORATORY

CALIFORNIA INSTITUTE OF TECHNOLOGY

PASADENA 3, CALIFORNIA

NOVEMBER 30, 1955

①

Contract No. AF 33(616)-3066  
Department of the Air Force

Progress Report No. 26-2

**CORROSION AND IGNITION OF TITANIUM ALLOYS IN FUMING NITRIC ACID  
II. STUDY OF ADDITIONAL CHEMICAL AND METALLURGICAL FACTORS**

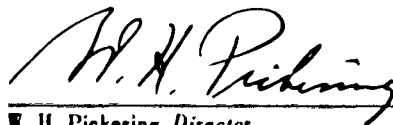
John B. Rittenhouse  
Stephen P. Vango  
Julia S. Whittick



David Altman, Chief  
Chemistry and Physics Section



for Arthur J. Stonick, Chief  
Rockets and Materials Division



W. H. Pickering, Director  
Jet Propulsion Laboratory

Copy No. 50

JET PROPULSION LABORATORY  
California Institute of Technology  
Pasadena 3, California  
November 30, 1955

### **NOTICES**

When Government drawings, specifications, or other data are used for any purpose other than in connection with a definitely related Government procurement operation, the United States Government thereby incurs no responsibility nor any obligation whatsoever; and the fact that the Government may have formulated, furnished, or in any way supplied the said drawings, specifications, or other data, is not to be regarded by implication or otherwise as in any manner licensing the holder or any other person or corporation, or conveying any rights or permission to manufacture, use, or sell any patented invention that may in any way be related thereto.

The information furnished herewith is made available for study upon the understanding that the Government's proprietary interests in and relating thereto shall not be impaired. It is desired that the Judge Advocate (WCJ), Wright Air Development Center, Wright-Patterson, Air Force Base, Ohio, be promptly notified of any apparent conflict between the Government's proprietary interests and those of others.

This document may not be reproduced or published in any form in whole or in part without prior approval of the Government. Since this is a progress report the information herein is tentative and subject to changes, corrections, and modifications.

✓

## TABLE OF CONTENTS

	Page
I. Introduction .....	1
II. Experimental Procedure .....	2
A. Laboratory Corrosion Studies .....	2
B. Ignition Studies .....	2
C. Sensitivity Studies .....	2
D. Heat Treatment of Samples .....	3
III. Results and Discussion .....	3
A. Effect of Composition of FNA, Surface Preparation, and Alloy Composition of Samples on Corrosion Rate .....	3
1. Role of $\text{NO}_2$ and $\text{H}_2\text{O}$ in acid on corrosion rates .....	3
2. Effect of surface preparation on corrosion rate .....	5
3. Effect of alloy composition on corrosion rates .....	5
B. Effect of Composition of FNA on Stress-Corrosion Cracking .....	6
1. Stress cracking on commercially pure titanium .....	6
2. Stress-corrosion cracking of the titanium-manganese alloy .....	7
3. Effect of liquid $\text{NO}_2$ on stress-corrosion cracking .....	7
C. Nature and Sensitivity of Black Coating .....	8
1. Analysis of coating .....	8
2. Impact sensitivity of black coating .....	9
3. Probing-sensitivity tests .....	9
D. Effect of Metallurgical History on Type of Corrosion Attack .....	10
1. Type of corrosion attack on annealed commercially pure titanium .....	10
2. Type of corrosion attack on annealed Ti -- 8% Mn sheet .....	10
3. Type of corrosion attack on heat-treated Ti -- 8% Mn sheet .....	11

## TABLE OF CONTENTS (Cont'd)

	Page
IV. Summary and Conclusions .....	13
V. Work in Progress and Future Work .....	13
Tables .....	15
Figures .....	22
References .....	29

## LIST OF TABLES

I. Average Corrosion Rates of Commercially Pure Titanium in FNA at 30°C with Surface As Received .....	15
II. Corrosion Rates of Commercially Pure Titanium in FNA at 30°C with Surface Sandblasted .....	16
III. Effect of Surface Preparation on Corrosion Rates of Some Titanium Alloys at Ambient Temperature .....	17
IV. Corrosion Rates of Ti -- 8% Mn Alloy in FNA at 30°C with Surface As Received .....	18
V. Corrosion Rates of Ti -- 8% Mn Alloy in FNA at 30°C with Surface Sandblasted .....	19
VI. Corrosion Rates and Chemical Analysis of Corrosion Product from Commercially Pure Titanium in FNA at Ambient Temperature .....	20
VII. X-ray Diffraction Pattern of Corrosion Product from Commercially Pure Titanium After Exposure to FNA .....	21

## LIST OF FIGURES

1. Average Corrosion Rates of Commercially Pure Titanium in FNA at 30°C, Surface As Received .....	22
2. Average Corrosion Rates of Commercially Pure Titanium in FNA at 30°C, Surface Sandblasted .....	22
3. Average Corrosion Rates of Ti -- 8% Mn Alloy in FNA at 30°C, Surface As Received .....	23

## LIST OF FIGURES (Cont'd)

	Page
4. Average Corrosion Rates of Ti -- 8% Mn Alloy in FNA at 30°C, Surface Sandblasted .....	23
5. Photomicrograph of Longitudinal Section of Commercially Pure Titanium Sheet (250X) .....	24
6. Photomicrograph of Transverse Section of Commercially Pure Titanium Sheet with 263 Hours Prior Exposure to 20% NO <sub>2</sub> Anhydrous FNA (250X) .....	24
7. Photomicrograph of Longitudinal Section of Ti -- 8% Mn Alloy (250X) .....	25
8. Photomicrograph of Transverse Section of Ti -- 8% Mn Alloy with 48 Hours Prior Exposure to 20% NO <sub>2</sub> Anhydrous FNA (150X) .....	25
9. Photomicrograph of Longitudinal-Edge Section of a Portion of the Sample of Figure 8, Unetched (250X) .....	26
10. Photomicrograph of Corner of Ti -- 8% Mn Sheet. Sample Heated in Vacuum ¼ Hour at 788°C, Quenched While in Vacuum into Liquid Nitrogen. Exposed to 20% NO <sub>2</sub> Anhydrous FNA for 24 Hours, Unetched (250X) .....	26
11. Photomicrograph of Base of Crack in Sample Shown in Figure 10, Etched (250X) .....	27
12. Photomicrograph of Transverse Section of Ti -- 8% Mn Alloy with Treatment Similar to Figure 10, Oblique Illumination, Etched (250X) .....	27
13. Same Section as Figure 12 but with Polarized Light .....	28
14. Photomicrograph of Ti -- 8% Mn Heated in vacuo to 788°C, Quenched into Ice Water, All-Beta Phase, Etched (250X) .....	28

## ERRATA FOR PROGRESS REPORT NO. 26-1

Page vi, Figure 8: For photomacrograph read photomicrograph

Page 6, line 7: For NO<sub>2</sub> to NO<sub>2</sub><sup>+</sup> and NO<sub>3</sub><sup>-</sup>, read NO<sub>2</sub> to NO<sup>+</sup> and NO<sub>3</sub><sup>-</sup>

Page 7, line 24: For 50 times read 5 times

Page 18, Figure 8: For photomacrograph read photomicrograph

Page 19, Figure 10: For 50X read 5X

### ABSTRACT

↓ The corrosion product removed from commercially pure titanium after exposure to 20%  $\text{NO}_2$  anhydrous fuming nitric acid was found by X-ray diffraction and chemical analysis to be titanium metal.

Metallographic observations indicate that the possible mechanism of corrosive attack of the fuming nitric acid on titanium and titanium alloys is through intergranular corrosion of the all-alpha or all-beta titanium alloys. Similar observations of the mixed alpha-beta alloy indicate a possible galvanic or electrochemical mechanism of the attack by liquid-phase fuming nitric acid. ↑

### I. INTRODUCTION

Corrosion is manifested in a number of ways dependent upon the corrosion environment and the metal or alloy exposed. Of the many manifestations of corrosion, three are considered of importance in the reaction of titanium and titanium alloys to fuming nitric acid (FNA).

The first, galvanic or electrochemical corrosion, has been defined in Reference 1 as a short-circuited couple of dissimilar metals or alloys in a corrosive medium as the electrolyte, or as macroscopic or microscopic areas within a metal dissimilar in composition or structure; an electric current is induced between electrodes, the electrode with the more anodic solution potential is dissolved while the other (more cathodic electrode) is relatively unattacked.

The second possible mode of corrosive attack, stress-corrosion cracking, is defined by Reference 1 as: "spontaneous failure of metals by cracking under combined action of corrosion and stress, residual or applied."

The third corrosion mechanism, intercrystalline corrosion, is described (Cf. Ref. 2) as preferential electrochemical attack of the grain boundaries due to precipitation or agglomeration in the grain boundary regions of phases or contaminants anodic to the grain interiors.

Considerable research effort has gone into the determination of the mechanism of stress-corrosion cracking (Cf. Ref. 3). The findings summarized are that tensile stresses are required to open crevices along localized paths of electrochemical corrosion where the localized paths are anodic areas and the surrounding metal is cathodic. The localized paths can be either intergranular or transgranular depending upon conditions in both the corrosive medium and the



exposed material (Cf. Ref. 4). According to Evans (Cf. Ref. 2), a large cathode-to-anode ratio will intensify intergranular corrosion if the material in the grain boundaries is anodic to the cathodic grain interior. A large cathode-to-anode ratio will increase galvanic corrosion attack by increasing the current density on the smaller anodic area (Cf. Ref. 5).

## **II. EXPERIMENTAL PROCEDURE**

### **A. Laboratory Corrosion Studies**

The apparatus consisting of glass tubes with a ground taper joint to which was fitted a stopcock with ball-joint tube (Cf. Ref. 6) was used for additional experiments to determine the effect of surface preparation of the titanium samples upon corrosion rates. Samples of titanium and titanium alloys approximately 0.5-inch square and 0.020- to 0.040-inch thick were sandblasted, using a 500-mesh-aluminum-oxide abrasive. Tank nitrogen at 50 psi was used as a carrier for the abrasive. The sandblasting was done immediately prior to weighing of the samples before exposure to the FNA. In order to remove any adhering grit, the samples were thoroughly blasted with a stream of clear tank nitrogen and then carefully brushed with a camel's-hair brush. This surface-preparation method has now been standardized for all samples before exposure to FNA.

### **B. Ignition Studies**

Samples exposed to FNA containing 20%  $\text{NO}_2$ , <sup>a</sup> 0%  $\text{H}_2\text{O}$ , and the remainder  $\text{HNO}_3$  for varying periods of time were subjected to probing tests for sensitivity to an ignition reaction. The sensitized sample was moistened with a small drop of FNA and the moistened surface was probed with a jeweler's screwdriver with a small, hardened-steel screwdriver bit. Other FNA-moistened samples were probed with a Tesla coil. Some sensitized samples, both dry and moistened with FNA, were heated in glass-working blast burner flame.

### **C. Sensitivity Studies**

Some of the dark coating was removed from sensitized samples by carefully scraping with a sharp knife. Small quantities of the coating were tested in the calibrated-drop-weight impact tester for sensitivity. Some of the material was tested dry and some of the material was tested after moistening with a drop of FNA.

---

<sup>a</sup> Unless otherwise stated, all percentage values are in wt %.

Small quantities of the scraped-off dark coating were exposed to the discharge of a Tesla coil.

#### D. Heat Treatment of Samples

Several of the samples were vacuum-annealed. The samples were placed in Vycor tubes which were evacuated during the heating cycle. As soon as the vacuum, as determined by Pirani gauge, reached  $10^{-5}$  mm of Hg, the tubes containing the samples were sealed off. Vacuum was maintained by a mechanical oil pump and an oil-diffusion pump. Temperatures were recorded and controlled by a chromel-alumel thermocouple and a Leeds and Northrup recording-indicating potentiometer. Holding time at temperature was  $\frac{1}{2}$  hour. The cooling rates were  $93^{\circ}\text{C}$  ( $200^{\circ}\text{F}$ ) per hour for the slowly cooled samples, a quench into liquid nitrogen with the samples still sealed in Vycor tube for intermediate cooling rates, and a quench into ice water by breaking the Vycor tube for a rapid cooling rate.

For the metallography of the samples, standard specimen-preparation techniques were used. The etchant used on those samples which were etched for photomicroscopy was 1 part HF and 1 part concentrated  $\text{HNO}_3$  in 2 parts glycerol. In order to protect the edges of the transverse sections, the samples were carefully clamped between sheets of copper before mounting in bakelite or transoptic mounts.

### III. RESULTS AND DISCUSSION

#### A. Effect of Composition of FNA, Surface Preparation, and Alloy Composition of Samples on Corrosion Rate

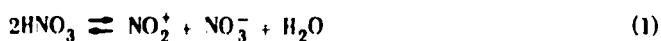
1. *Role of  $\text{NO}_2$  and  $\text{H}_2\text{O}$  in acid on corrosion rate.* The anomalous behavior of commercially pure titanium in 10%  $\text{NO}_2$  FNA in the as-received condition discussed in Figure 3 of Reference 6 has been resolved. The results from two repeated experiments of one-week duration involving exposure of the commercially pure as-received titanium is shown in Figure 1. These are average values from duplicate samples in each experiment.

The effect of  $\text{H}_2\text{O}$  on the corrosion rate is most pronounced in the case of the FNA containing 20%  $\text{NO}_2$ . Here the corrosion rate drops from approximately 1.9 mils/yr at 0%  $\text{H}_2\text{O}$  to 0.12 mil/yr at 1.0%  $\text{H}_2\text{O}$  to 0.043 mil/yr at 2.0%  $\text{H}_2\text{O}$ .

Considering now the effect of  $\text{NO}_2$  in Figure 1, one can see that the corrosion rate in 10%  $\text{NO}_2$  and 0%  $\text{H}_2\text{O}$  FNA is 0.09 mil/yr, whereas at 1% water, the rate drops slightly to 0.052 mil/yr.

There is then a slight increase in corrosion rate as the  $H_2O$  content is increased to 2.0%; the rate here is 0.08 mil/yr. A similar effect is noted with the curve for FNA containing 0%  $NO_2$  as the  $H_2O$  content is increased.

As discussed in Reference 6, the possible mechanism of corrosion is by  $NO_2^+$  ion and  $NO_2$  species in FNA solutions containing small concentrations of  $H_2O$ . As the  $H_2O$  content is increased, the equilibrium of Equation 1 is shifted to the left with a reduction in concentration of  $NO_2^+$  and  $NO_3^-$

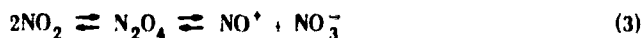


This equation expresses the self-ionization of  $HNO_3$ . As the  $H_2O$  content approaches 3.0%, another ionization mechanism is effective, as indicated in Equation (2)



This latter reaction can account for the slight increase in corrosion rate seen in Figure 1 as the  $H_2O$  content is increased to 2%

The fact that  $NO_2$  in nitric acid solution ionizes as follows:



would lead one to hypothesize that  $NO^+$  ion contributes to the corrosion reaction; however, it was shown previously (Cf. Ref. 6) that corrosion rates were highest when 1.25%  $N_2O_5$  was added to anhydrous FNA. From the following equilibrium, it can be reasoned that  $NO_2^+$  or  $NO_2$  probably are the species responsible for the corrosive attack (Cf. Refs. 6 and 7):



According to Reference 7, electrical conductivity of the FNA increases with increasing  $NO_2$  and decreases with increasing  $H_2O$  in the range of  $H_2O$  content from 0 to 3.5%. The electrochemical theories of corrosion are fairly well established (Cf. Ref. 2). One can then postulate that the increasing conductivity of the corrosion medium with increasing  $NO_2$  concentration can account for the increase in corrosion observed in Figure 1. Table I shows the average corrosion rates for one of the experimental runs plotted in Figure 1.

2. *Effect of surface preparation on corrosion rate.* In Figure 2 the average corrosion rates of commercially pure titanium in FNA at 30°C after the surfaces of the samples had been sandblasted are plotted against the percentage of  $H_2O$  in the FNA. Comparing the corrosion rates of Figure 2 with those of Figure 1 where the samples were not sandblasted, one can see that the corrosion rates of the sandblasted samples are slightly higher than the corresponding corrosion rates of the not-sandblasted samples. The corrosion rates plotted in Figure 2 are tabulated in Table II.

Commercial titanium and titanium alloys are rolled and annealed at relatively high temperatures in air. Titanium has a high affinity for oxygen (Cf. Ref. 8); therefore, an oxide film or possibly residual scale can exist on the surface of the sheet even after pickling. It is doubtful if this entire oxide surface is removed by sandblasting. There is the possibility that a new oxide coating forms almost immediately after sandblasting (Cf. Ref. 8). However, it is possible that sandblasting produces enough surface roughness to supply small discontinuities in the oxide surface layer for subcutaneous access of the FNA. As mentioned in Section II-A of this report, sandblasting immediately prior to sample weighing before exposure to FNA has been standardized for sample surface preparation. This method, it is believed, will develop a reasonably reproducible surface on all samples.

Table III shows the data from a preliminary study of the effect of surface preparation on the corrosion rates of commercially pure titanium and the titanium-manganese<sup>a</sup> alloy. As can be seen, the corrosion rates for the sandblasted samples and the rates for the polished samples were higher than the rates for the as-received samples. The polished samples were polished on metallographic polishing papers to 500-mesh abrasive immediately before weighing prior to exposure to the FNA. It can be noticed in Table III that the corrosion rates for the polished and for the sandblasted samples of titanium-manganese alloy are almost identical. The rates for the commercially pure titanium in the parallel conditions are not identical. That is, the corrosion rate of the sandblasted samples is higher than the rate for the polished samples. The reason for this behavior is not understood at this time.

3. *Effect of alloy composition on corrosion rates.* The data for the corrosion rates of samples of the titanium-manganese alloy in the as-received condition and in the sandblasted condition are tabulated in Tables IV and V, and these data are plotted in Figure 3 and 4. The effects of  $NO_2$  and water in FNA are similar for this alloy to the effects of these species on the commercially pure titanium, as shown in Figure 1 and 2. That is,  $NO_2$  increases the corrosion rates, whereas  $H_2O$  decreases the corrosion rates. This relationship is not consistent over the

---

<sup>a</sup> In this report, the titanium-manganese alloy referred to is the binary alloy of titanium containing nominally 8% manganese.

entire range of composition, however, for it can be seen in Figures 3 and 4 that at 2%  $H_2O$  the corrosion rates in FNA containing 0%  $NO_2$  are slightly higher than those rates in FNA containing 10%  $NO_2$ , and these in turn are slightly higher than in FNA containing 20%  $NO_2$ .

The effect of surface preparation is not as consistent with the titanium-manganese alloy as this effect is with the commercially pure titanium. In the case of the 20%  $NO_2$  anhydrous FNA, the corrosion rates for the sandblasted samples are higher than the rates for the as-received samples. This effect is consistent with the results of Table III. The corrosion rates in FNA containing 1% and 2%  $H_2O$  of samples in the sandblasted condition are slightly higher than those as-received samples in FNA of comparable compositions. However, the difference in rates between as-received and sandblasted samples is not as marked in the Ti-Mn alloy as in the commercially pure Ti.

It is in the anhydrous FNA where the effect of alloy composition is most marked. In both the sandblasted and as-received condition the corrosion rates of the manganese-bearing alloy are somewhat higher than corresponding rates for the commercially pure titanium.

There is a possibility that these higher corrosion rates of the titanium-manganese alloy in anhydrous FNA containing 10 to 20%  $NO_2$  may be responsible for the more consistent ignition reactions obtainable with this alloy since higher corrosion rates would presuppose a larger volume of corrosion products except where stress-corrosion cracking is a factor. Under stress-corrosion-cracking conditions, much of the corrosion product is probably concentrated in the localized area of the crack, although some corrosion product may appear on the sample surface.

It is also considered that the higher corrosion rates of the titanium-manganese alloy in anhydrous FNA containing 10 to 20%  $NO_2$  may be associated with the higher electrical conductivity of this acid (Cf. Ref. 9). This higher electrical conductivity of the corrosion medium may set up higher electrochemical currents between anodic and cathodic regions of the alloy and possibly increase the intensity of the corrosion of the anodic regions.

## B. Effect of Composition of FNA on Stress-Corrosion Cracking

1. *Stress cracking of commercial pure titanium.* Stress-cracked samples have been noted in Tables I to III and in Figures 1 and 2. Commercially pure titanium will stress-crack around identifying numbers stamped on the samples. Some of these stress-corrosion cracks may originate in the sheared edges of the samples. This stress-cracking only occurs in anhydrous FNA and only in anhydrous FNA containing 10 to 20%  $NO_2$ . The exact lower limit of  $NO_2$  content to produce stress cracking has not been ascertained.

2. *Stress-corrosion cracking of the titanium-manganese alloy.* In Tables III through V and in Figures 3 and 4 are noted those samples of Ti-Mn alloy that showed stress-corrosion cracking. The effect of the FNA composition on the stress-corrosion cracking of the titanium-manganese alloy is comparable to the results obtained with the commercially pure titanium with one exception. That is, in the case of the titanium-manganese alloy stress-corrosion cracking, as indicated by fractures around identifying numbers stamped into the samples, occurred in FNA containing 0%  $\text{NO}_2$  and 0%  $\text{H}_2\text{O}$  in those samples which were not sandblasted. The sandblasted samples exposed to FNA containing 0%  $\text{NO}_2$  and 0%  $\text{H}_2\text{O}$  did not exhibit stress-corrosion cracking.

This borderline behavior with respect to stress-corrosion cracking of the titanium-manganese alloy in anhydrous FNA containing 0%  $\text{NO}_2$  cannot be explained at this time. However, there is a possible indication that the stress-corrosion mechanism is probably due to the higher corrosion rates associated with the anhydrous FNA and therefore the  $\text{NO}_2^+$  ion.

3. *Effect of liquid  $\text{NO}_2$  on stress-corrosion cracking.* An experiment to clarify the  $\text{NO}_2$  effect on the commercially pure titanium and the titanium-manganese alloy was performed. Duplicate samples of each material were immersed in purified  $\text{NO}_2$  in a glass tube; the assembly was frozen in liquid nitrogen and evacuated. The glass tube was sealed off. This procedure then allowed the  $\text{NO}_2$  to remain liquid under its own vapor pressure at room temperature. After 44 hours of exposure of the samples to the liquid  $\text{NO}_2$ , the corrosion rates were found to be 0.32 mil/yr for the commercially pure titanium and 0.20 mil/yr for the titanium-manganese alloy. There were no stress-corrosion cracks on any of the samples so exposed. These samples were probed for ignition sensitivity and were found to be insensitive.

While this experiment does not conclusively prove that  $\text{NO}_2$  species in FNA is not responsible for either stress-corrosion cracking or the production of the ignition-sensitive coating on the samples, it does prove that liquid  $\text{NO}_2$  itself does not cause ignition-sensitive reactions or stress-corrosion cracking in commercially pure titanium and the titanium-manganese alloy.

The indications are that commercially pure titanium is susceptible to stress-corrosion cracking in anhydrous FNA containing 10 to 20%  $\text{NO}_2$ . It is further indicated that the titanium-manganese alloy exhibits borderline susceptibility to stress-corrosion cracking in anhydrous FNA containing 0%  $\text{NO}_2$ . The titanium-manganese alloy is susceptible to stress-corrosion cracking in anhydrous FNA containing 10 to 20%  $\text{NO}_2$ .

Based on present results, however, commercially pure titanium and the titanium-manganese alloy are not susceptible to stress-corrosion cracking in FNA in the concentration ranges 0 to 20%  $\text{NO}_2$  and 1 to 2%  $\text{H}_2\text{O}$ .

### C. Nature and Sensitivity of Black Coating

1. *Analysis of coating.* Large samples (about 1 x 1/2 inch) of commercially pure titanium were immersed in 20% NO<sub>2</sub> anhydrous FNA at ambient temperature. The samples were carefully weighed after sandblasting and before exposure. These samples were exposed for periods of time that were considered long enough to develop a large quantity of the dark coating for chemical and X-ray analysis. After exposure, the samples were reweighed. Then the dark corrosion product was carefully scraped from the surface under water to avoid explosion hazard. After drying, the dark powder obtained was analyzed both chemically and by X-ray diffraction. Table VI shows the results of the chemical analysis which indicate that the black corrosion product which was developed after exposure of commercially pure titanium to anhydrous FNA containing 20% NO<sub>2</sub> was very nearly all titanium metal. It is shown in Section III-B that this material was sensitive to ignition reactions.

The X-ray diffraction analysis of the dark-corrosion-product powder is shown in Table VII. The diffraction pattern was obtained on General Electric XR1D3 X-ray diffraction equipment, a Debye-Scherrer powder diffraction camera of 143.2-mm diameter was used with a copper target diffraction X-ray tube. The radiation was filtered with a nickel foil. The diffraction film was measured on a comparator and the line intensities were estimated.

The X-ray diffraction pattern showed the strong lines characteristic of the hexagonal close-packed crystal structure of alpha titanium (Cf. Ref. 10). There were some very faint diffraction lines superimposed on the characteristic alpha-titanium lines. Table VII shows an attempt to tentatively identify the possible compounds which could account for these superimposed diffraction lines. From the literature (Cf. Ref. 11) one can postulate that any oxygen or nitrogen present in relatively small quantities in commercially pure titanium will be dissolved in the alpha matrix. Carbon, probably as TiC, however, has a very limited solubility in the alpha matrix, so titanium carbides could reside in the grain boundaries. These were not detected, however. With hydrogen reported in the commercially pure titanium at the level of 0.004% H<sub>2</sub> (Cf. Ref. 6) there is a possibility of TiH<sub>2</sub> in the microstructure as discussed by Craighead, Lenning, and Jaffee (Cf. Ref. 12). TiH<sub>2</sub> has been tentatively identified in the X-ray diffraction pattern, and in Section III-C of this report TiH<sub>2</sub> line markings similar to those observed by Craighead, Lenning, and Jaffee can be seen.

The X-ray diffraction analysis then confirms the chemical analysis. That is, the dark coating removed from the commercially pure titanium exposed to FNA containing 20% NO<sub>2</sub> and 0% H<sub>2</sub>O was predominantly titanium metal present on the sample surface in a finely divided state.

The fact that a finely divided metal can undergo ignition reactions is not entirely unusual. Kroll (Cf. Ref. 13) has reported that powdered zirconium is pyrophoric and reacts violently with moisture under shock. Larsen et al have reported ignition reactions (Cf. Ref. 14) involving

uranium-zirconium alloys with nitric acid. The alloy composition range was 1 to 50% zirconium, and the nitric acid composition ranged from 8 to 16 molar. The investigation (Cf. Ref. 14) concluded that unoxidized particles of an epsilon phase containing from 55 to 81 atomic % zirconium was the material reacting violently.

2. *Impact sensitivity of black coating.* The impact sensitivity of the black coating removed from samples that had been stored in FNA containing 20%  $\text{NO}_2$  and 0%  $\text{H}_2\text{O}$  was determined by using a calibrated drop-weight-testing apparatus (Cf. Ref. 15). The dry powder did not react to an impact load that would cause TNT to explode. This fact implies then that the dry powder is not as sensitive to explosion by impact as TNT.

On the other hand, samples of the powder moistened with FNA (14%  $\text{NO}_2$  and 2%  $\text{H}_2\text{O}$ ) did have an impact sensitivity equal to that of nitroglycerine or mercury fulminate (Cf. Ref. 15).

3. *Probing-sensitivity tests.* Additional samples of commercially pure titanium and the titanium-manganese alloy which had been exposed to anhydrous FNA containing 20%  $\text{NO}_2$  for periods of from 24 to 48 hours were tested for ignition sensitivity by probing with a hardened-steel tool. The intensity of the ignition reaction as judged by amount of flash varied, depending upon the amount of sensitive dark coating on the sample and also upon the presence of nitric acid (acid compositions ranging from concentrated, i. e., 70%  $\text{HNO}_3$ , to FNA containing 14%  $\text{NO}_2$  and 2%  $\text{H}_2\text{O}$ ). The nature of the ignition reaction can be described as from mild to violent. The mild reaction gives rise to sparks only, whereas the violent one gives rise to a bright flash accompanied by a loud report. When the samples were not moistened with nitric acid or FNA, only sparks were produced upon probing. When the samples were moistened with nitric acid or FNA, the intensity of the ignition was dependent upon the thickness of the dark coating on the sample.

◦ Samples that had not received prior sensitizing treatment in 20%  $\text{NO}_2$  anhydrous FNA exhibited no ignition reactions of any degree when probed with a hardened-steel tool.

The results of probing tests using a Tesla coil were comparable with similar tests using the hardened-steel probe. It was found also that the black powder scraped off of samples that had prior exposure to 20%  $\text{NO}_2$  anhydrous FNA gave off sparks when either dry or moistened with FNA under the Tesla-coil discharge.

A sample of heat-treated titanium-manganese alloy that had been exposed to 20%  $\text{NO}_2$  anhydrous FNA for 48 hours was quarter-sectioned. This sample developed a very heavy coating of black corrosion product. One quarter section of the sample was probed with a hardened-steel tool without moistening the sample with FNA; sparks were emitted. A second quarter of the sample was probed after being moistened with FNA (14%  $\text{NO}_2$  and 2%  $\text{H}_2\text{O}$ ); a bright flash



accompanied by a loud report resulted. Only that portion of the sample which had been moistened with FNA was discolored by the ignition reaction. A third section of the quartered sample which was not moistened with FNA was heated in the flame of a glass-working blast burner. Although the piece was heated to redness, no ignition reaction occurred, and there was no afterglow. The fourth quarter was moistened with FNA and then heated in the blast-burner flame to redness; there was no ignition reaction and no afterglow.

#### D. Effect of Metallurgical History on Type of Corrosion Attack

1. *Type of corrosion attack on annealed commercially pure titanium.* In Figure 5 there is reproduced a photomicrograph of a longitudinal section of a piece of commercially pure titanium. This photomicrograph shows the typical equiaxed microstructure of a hot-worked and annealed commercially pure metal. The needlelike line markings are attributed to  $TiH_2$  by Craighead et al (Cf. Ref. 12). The clear globules within the grains are probably a small quantity of retained beta-phase in the alpha matrix. The very dark etching spots have not been identified but could be titanium carbides.

The photomicrograph shown in Figure 6 is a transverse section through a piece of commercially pure titanium sheet that had been exposed to 20%  $NO_2$  anhydrous FNA for 263 hours. The upper portion of the photomicrograph is a piece of copper sheet in which the titanium sheet was clamped to protect the edge of the titanium sheet during metallographic preparation. It would appear that the corrosive attack was intergranular. This intergranular attack could account for the presence of titanium metal found in both the chemical and X-ray diffraction analysis of the dark coating removed from the commercially pure titanium samples.

2. *Type of corrosion attack on annealed Ti - 8% Mn sheet.* The photomicrograph of Figure 7 was from a longitudinal section of a piece of annealed Ti - 8% Mn sheet. This alloy has a mixed alpha-beta structure in the hot-rolled and annealed condition (Cf. Ref. 16). In Figure 7 the alpha phase is the grey half-tone portions, while the clear portions of the photomicrograph are the beta phase.

At 150 diameters in Figure 8 is reproduced a transverse section through a sample of Ti - 8% Mn alloy that had received prior treatment for 48 hours in 20%  $NO_2$  anhydrous FNA. The top of the photomicrograph is of a piece of copper sheet used to protect the edge of the titanium sample during polishing. The mottled dark area approximately 1-cm thick on the photomicrograph is probably the ignition-sensitive, dark corrosion product. A longitudinal-edge section of a piece of the same sample unetched is shown in Figure 9 at a magnification of 250 times. The deep black portion of this photomicrograph is the bakelite mounting in which the sample section was embedded for ease in handling during metallographic preparation. The mottled dark section has the appearance of the ignition-sensitive coating.

The appearance of the corroded layers of these alpha-beta Ti - 8% Mn alloy samples suggests the possibility of selective or galvanic attack by the FNA on one of the phases of the alloy. It is postulated that the beta phase is anodic to the alpha phase in FNA. One can theorize that the beta phase containing most of the manganese in solid solution (Cf. Ref. 17) is preferentially attacked; the alpha phase, being nearly pure titanium, is possibly cathodically protected in the presence of the beta phase and may present a fresh surface in finely divided state in the corrosion product which when heated by a friction force or impact in the presence of a strong oxidizer such as FNA can possibly react violently.

3. *Type of corrosion attack on heat-treated Ti - 8% Mn sheet.* It may be considered that the distribution of the alpha and beta phases in the alloy may have some influence on the mode and extent of the corrosive attack of the FNA on the Ti - 8% Mn material. Two heat treatments that would markedly alter the distribution of the alloy microconstituents were carried out.

The first heat treatment involved a cooling rate from the all-beta temperature that would produce a Widmanstätten distribution of the alpha in the beta matrix (Cf. Refs. 17 and 18). Four pieces of Ti - 8% Mn sheet 0.5 x 0.5 x 0.02 inch were placed in a Vycor tube. The tube was evacuated to  $10^{-5}$  mm Hg during the heating cycle. The tube was then sealed off. After  $\frac{1}{2}$  hour at 788°C (1450°F) the tube containing the samples was quenched into liquid nitrogen without breaking the Vycor tube. The samples were then removed from the Vycor tube and were sand-blasted and weighed before exposure to 20% anhydrous FNA for 24 hours. These samples were probed for ignition sensitivity after exposure to the FNA and were found to produce violent ignition reactions. An unetched photomicrograph at 250X of one corner of a longitudinal section of one of the samples treated in this manner is shown in Figure 10. A photomicrograph of the base of the crack shown in Figure 10 is shown in the etched photomicrograph of Figure 11. In Figure 11, the grain boundaries are outlined by alpha. Within the grains the needlelike alpha has precipitated upon preferred planes of the beta matrix. Notice that the intercrystalline corrosion attack has avoided the alpha in the grain boundary and has followed the grain outline in the beta matrix.

A possible explanation of this behavior can be obtained from a study of the titanium-manganese phase diagram (Cf. Ref. 17). The maximum solubility of manganese in alpha titanium at the eutectoid temperature (550°C) is 0.5%. The eutectoid concentration of manganese in beta titanium at the eutectoid temperature is 20%. Precipitation of the nearly pure alpha titanium at the beta grain boundary can cause an enrichment in manganese of the beta grain in the region adjacent to the precipitated alpha phase. This manganese enrichment in the region adjacent to the precipitated alpha could constitute a concentration gradient which would increase the anodic solution potential at those regions and thus promote intergranular corrosion attack.

This behavior would be somewhat analogous to the intergranular corrosion of certain of the stainless steels (Cf. Ref. 19). Although in the stainless steels the mechanism is an impoverishment of chromium which causes an increase in the solution potential of the iron matrix, it is reasonable that the opposite or enrichment effect postulated for the titanium-manganese alloy can occur. Two additional photomicrographs of a transverse section of a similarly treated sample are shown in Figures 12 and 13. Oblique illumination was used on the etched sample in Figure 12, while polarized light was used in the photomicrograph of Figure 13. It is interesting to note the continuing grain boundary in Figure 13 as it proceeds into the corroded layer. The corroded layer is obscured in the very dark portion of Figure 12. Under polarized light the beta phase remains dark, while the alpha phase is bright in titanium alloys when the sample is rotated about the optical axis of the microscope (Cf. Ref. 20). It is possible that the intergranular attack shown in Figures 10 and 11 may be stress-corrosion cracking, however, the general appearance of the attack was characteristic of intergranular corrosion.

The second heat treatment used was a drastic quench to preserve the beta phase at room temperature. Three samples were heated *in vacuo* in Vycor tubing to 788°C (1450°F) and held for ¼ hour at temperature. The Vycor tube with the samples was sealed off with a vacuum of  $10^{-5}$  mm Hg. In the cooling cycle, the Vycor tube with the samples was broken below the surface of an ice-water quenching bath. This cooling rate is sufficient to retain the beta phase at room temperature in the Ti - 8% Mn alloy (Cf. Refs. 16 and 18). Two of the samples thus treated were sandblasted, weighed, and exposed to 20% NO<sub>2</sub> anhydrous FNA for 24 hours.

The photomicrograph of Figure 14 is an etched longitudinal section of an edge of one of the samples treated as described above. It appears that the corrosive mechanism on the all-beta titanium-manganese alloy was by intergranular corrosion or stress-corrosion cracking.

Tests on one of the samples thus treated resulted in violent ignition reactions when moistened with FNA (14% NO<sub>2</sub> and 2% H<sub>2</sub>O) and probed with a hardened steel tool. Corrosion rates of alpha-phase titanium should be essentially that of commercially pure titanium. The average rate for this material in 20% NO<sub>2</sub> anhydrous FNA from Table II is 4.8 mils/yr. Similarly, the average corrosion rate of the alpha-beta titanium is typical of that of the Ti - 8% Mn alloy in 20% anhydrous FNA as found in Table V or 30 mils/yr. A comparison of the average corrosion rates, in 20% NO<sub>2</sub> anhydrous FNA, of the Ti - 8% Mn alloy quenched to produce two different microstructures can be made. The average corrosion rate of the samples quenched to the two-phase Widmanstätten structure (Cf. Fig. 11) was 148 mils/yr, while the comparable rates of the samples quenched to the single-phase all-beta condition (Cf. Fig. 14) was 251 mils/yr. It is possible that part of the higher corrosion rates reported for the quenched alloys could be due to strain-accelerated corrosion or to stress-corrosion cracking. It is indicative, however, that the mechanism involving intergranular corrosion appeared to be true of both the alpha- and beta-phase titanium. Also, it should be pointed out that the mechanism seems to be anodic-cathodic corrosion of beta (anodic)

and alpha (cathodic) areas in the annealed (Cf. Fig. 8) and the intermediately quenched Ti -8% Mn alloy (Cf. Figs. 11, 12, and 13).

#### IV. SUMMARY AND CONCLUSIONS

A summary of the recent findings of the investigation of the corrosion and ignition reactions of titanium and titanium alloys in liquid phase FNA are as follows:

1. Generally, corrosion rates in FNA at 30°C of sandblasted samples were higher than samples not sandblasted.
2. The corrosion rates of the Ti - 8% Mn alloy samples in the annealed and sandblasted condition were higher than similar samples of commercially pure titanium in FNA at 30°C.
3. The annealed Ti - 8% Mn alloy samples showed stress-corrosion cracking in FNA containing 0% H<sub>2</sub>O and 10 to 20% NO<sub>2</sub>. Borderline-stress-corrosion-cracking susceptibility of this alloy was also exhibited in FNA containing 0% H<sub>2</sub>O and 0% NO<sub>2</sub>.
4. The probable mechanism of corrosion in the all-alpha or all-beta titanium alloy is by intergranular corrosion.
5. The postulated corrosion mechanism in the mixed alpha-beta alloy is electrochemical or galvanic corrosion of anodic-cathodic areas within the alloy.
6. The chemical and X-ray diffraction analysis of the black sensitive corrosion product removed from titanium samples exposed to 20% NO<sub>2</sub> anhydrous FNA was titanium metal.
7. The impact sensitivity of the black sensitive corrosion product removed from titanium samples exposed to 20% NO<sub>2</sub> anhydrous FNA was comparable to the impact sensitivity of nitroglycerine or mercury fulminate, provided the powder was moistened with FNA (14% NO<sub>2</sub> and 2% H<sub>2</sub>O). The dry powder was not as sensitive as TNT.

#### V. WORK IN PROGRESS AND FUTURE WORK

The following is a summary of the work in progress and the nature and direction of future work along the lines of the present investigation:

1. Work is in progress and will continue on the determination of the incubation time to produce the sensitive coating and the time to induce stress-corrosion cracking.
2. Investigation of the decomposition of the FNA and the analysis of some of the decomposition products after exposure of titanium to 20%  $\text{NO}_2$  anhydrous FNA is underway.
3. Corrosion rates of vacuum stress-relieved samples of both commercially pure titanium and Ti - 8% Mn alloy are being obtained.
4. A 30-day exposure test at 30°C in liquid-phase thermally stable FNA (14%  $\text{NO}_2$  and 3%  $\text{H}_2\text{O}$ ) has been started.
5. Further work on the effect of surface preparation on corrosion rates of titanium and titanium alloys in liquid-phase FNA has been scheduled.
6. A study of the precise critical concentrations of  $\text{H}_2\text{O}$  and  $\text{NO}_2$  in FNA to develop the ignition sensitivity is proceeding.
7. The effect of temperature on corrosion rates and the incubation time to produce the sensitive coating will be investigated.
8. The determination of the minimum stress to produce stress-corrosion cracking of titanium in liquid-phase FNA will be undertaken.
9. The effects of the gas phase of various concentrations of FNA on titanium and titanium alloys will be studied.

TABLE I  
AVERAGE CORROSION RATES OF COMMERCIAL PURE TITANIUM  
IN FNA AT 30°C WITH SURFACE AS RECEIVED

Sample Number	H <sub>2</sub> O (%)	NO <sub>2</sub> (%)	HNO <sub>3</sub> (%)	Corrosion Rate (mils/yr)	Stress Cracked
35	0	0	100	0.044	no
45	0	0	100	0.044	no
100	1	0	99	0.030	no
68	1	0	99	0.030	no
47	2.1	0	97.9	0.036	no
102	2.1	0	97.9	0.036	no
106	0	10.2	89.8	0.089	yes
90	0	10.2	89.8	0.089	yes
79	1.0	10.3	88.7	0.051	no
99	1.0	10.3	88.7	0.051	no
67	1.7	9.8	88.5	0.077	no
53	1.7	9.8	88.5	0.077	no
73	0	20.8	79.2	1.85	yes
52	0	20.8	79.2	1.85	yes
98	1.2	19.6	79.2	0.113	no
65	1.2	19.6	79.2	0.113	no
66	2.1	19.3	78.6	0.042	no
64	2.1	19.3	78.6	0.042	no

TABLE II  
CORROSION RATES OF COMMERCIALLY PURE TITANIUM IN FNA  
AT 30°C WITH SURFACE SANDBLASTED

Sample Number	H <sub>2</sub> O (%)	NO <sub>2</sub> (%)	HNO <sub>3</sub> (%)	Corrosion Rate (mils/yr)	Stress Cracked
236	0	0	100	0.133	no
225	0	0	100	0.133	no
229	1.2	0	98.8	0.163	no
233	1.2	0	98.8	0.097	no
207	2.1	0	97.9	0.093	no
214	2.1	0	97.9	0.136	no
205	0	10.2	89.8	0.383	yes
239	0	10.2	89.8	0.496	yes
220	1.0	10.3	87.7	0.296	no
228	1.0	10.3	87.7	0.153	no
201	1.7	9.8	88.5	0.147	no
222	1.7	9.8	88.5	0.183	no
200	0	19.8	80.2	3.80	yes
231	0	19.8	80.2	5.74	yes
206	1.2	19.6	79.2	0.147	no
219	1.2	19.6	79.2	0.137	no
216	2.1	19.3	78.6	0.177	no
247	2.1	19.3	78.6	0.197	no

**TABLE III**  
**EFFECT OF SURFACE PREPARATION ON CORROSION RATES OF SOME**  
**TITANIUM ALLOYS IN 20% NO<sub>2</sub> ANHYDROUS FNA AT AMBIENT**  
**TEMPERATURE FOR 118 HOURS**

Surface Treatment	Corrosion Rate (mils./yr)	Stress Cracked
Commercially Pure Titanium		
As received	3.4	yes
Sandblasted	4.9	yes
Polished	7.9	yes
Ti--8% Mn Alloy		
As received	17.1	yes
Sandblasted	51.2	yes
Polished	50.5	yes



TABLE IV  
CORROSION RATES OF Ti-8% $\text{Mn}$  ALLOY IN FNA AT 30°C WITH  
SURFACE AS RECEIVED

Sample Number	$\text{H}_2\text{O}$ (%)	$\text{NO}_2$ (%)	$\text{HNO}_3$ (%)	Corrosion Rate (mils yr)	Corrosion Cracked
52	0	0	100	0.622	yes
11	0	0	100	0.606	yes
89	1	0	99	0.065	no
82	1	0	99	0.135	no
66	2	0	98	0.135	no
87	2	0	98	0.103	no
67	0	10	90	6.76	yes
78	0	10	90	5.73	yes
38	1	10	89	0.092	no
6	1	10	89	0.103	no
93	2	10	88	0.097	no
8	2	10	88	0.108	no
47	0	20	80	27.85	yes
58	0	20	80	32.50	yes
21	1	20	79	0.059	no
49	1	20	79	0.087	no
63	2	20	78	0.059	no
90	2	20	78	0.059	no

**TABLE V**  
**CORROSION RATES OF Ti-8% Mn ALLOY IN FNA AT 30°C WITH**  
**SURFACE SANDBLASTED**

Sample Number	H <sub>2</sub> O (%)	NO <sub>2</sub> (%)	HNO <sub>3</sub> (%)	Corrosion Rate (mils/yr)	Stress Cracked
232	0	0	100	0.310	no
227	0	0	100	0.326	no
205	1.2	0	98.8	0.187	no
219	1.2	0	98.8	0.143	no
211	2.1	0	97.9	0.210	no
221	2.1	0	97.9	0.197	no
212	0	10.2	89.8	11.99	yes
226	0	10.2	89.8	12.99	yes
203	1.0	10.3	88.7	0.200	no
223	1.0	10.3	88.7	0.223	no
228	1.7	9.8	88.5	0.183	no
233	1.7	9.8	88.5	0.147	no
241	0	19.8	80.2	81.40	yes
242	0	19.8	80.2	62.8	yes
213	1.2	19.6	79.2	0.110	no
230	1.2	19.6	79.2	0.100	no
202	2.1	19.3	78.6	0.130	no
207	2.1	19.3	78.6	0.180	no

**TABLE VI**  
**CORROSION RATES AND CHEMICAL ANALYSIS OF CORROSION**  
**PRODUCT FROM COMMERCIAL PURE TITANIUM IN FNA**  
**AT AMBIENT TEMPERATURE**

Exposure Conditions	
Acid composition (%)	
NO <sub>2</sub>	20.8
H <sub>2</sub> O	0
HNO <sub>3</sub>	remainder
Time (hrs)	263
Corrosion Rates	
Sample A (mils/yr)	7.00
Sample B (mils/yr)	6.30
Analysis of Corrosion Product Removed from Samples A and B	
Coating in sample (mg)	2.40
Titanium in sample (mg)	2.34
Error or milligrams unaccounted for	0.06

**TABLE VII**  
**X-RAY DIFFRACTION PATTERN OF CORROSION PRODUCT FROM**  
**COMMERCIAL PURE TITANIUM AFTER EXPOSURE TO FNA**

$d, \text{\AA}$ observed	Observed intensity <sup>b</sup>	$d, \text{\AA}$ $\text{Ti}^c$	Intensity	$d, \text{\AA}$ $\text{TiH}_2^d$	$d, \text{\AA}$ $\text{TiN}^e$	$d, \text{\AA}$ $\text{TiO}^e$
					3.49	3.92
						3.29
						2.92
						2.755
2.56	M	2.56	40		2.58	
2.34	M	2.34	40	2.49		2.49
2.25	S	2.24	100	2.23	2.282	
2.09	VW				2.205	
2.03	VW			2.05	2.09	
1.97	VW					
1.87	VW					1.88
1.79	W					
1.73	W	1.73	40		1.784	1.724
1.60	VW			1.55		
1.47	W	1.48	40		1.514	
					1.448	1.437
1.37	VVW				1.388	1.418
1.334	W	1.34	50	1.344	1.369	1.361
1.249	W	1.25	40		1.29	
1.231	VW	1.23	30		1.261	1.26
					1.197	
1.166	VVW	1.18	10		1.18	
					1.164	
1.096	VVW	1.13	10		1.135	
		1.07	20		1.086	
				1.03	1.038	
				1.01	1.014	
0.944	VVW	0.99	30		1.002	
		0.94	30		0.954	
0.909	VVW	0.92	30	0.911	0.933	
0.88	VVW	0.88	10		0.902	
					0.85	
					0.84	
0.82	VVW				0.832	
					0.815	
					0.811	

<sup>a</sup>Interplanar spacing of atoms

<sup>b</sup>S = strong, M = medium, W = weak, VW = very weak, VVW = very very weak

<sup>c</sup>Cf. Ref. 10.

<sup>d</sup>Private communication of I. D. Jaffe, Chief, Materials Section, Jet Propulsion Laboratory.

<sup>e</sup>Cf. Ref. 11.

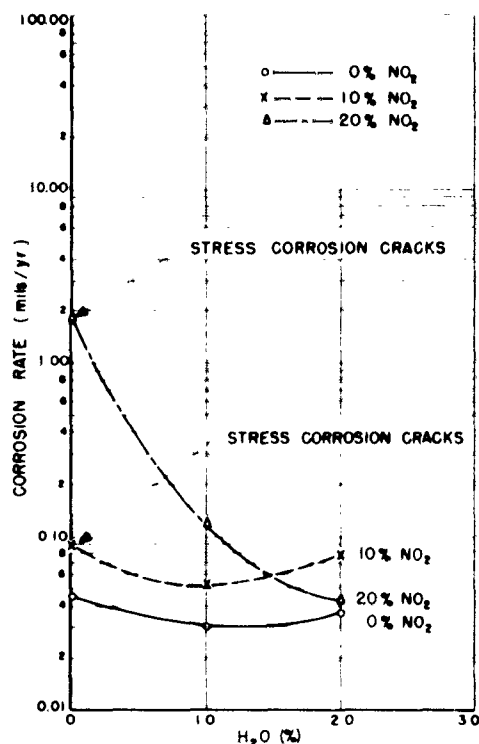


Figure 1. Average Corrosion Rates of Commercially Pure Titanium in FNA at 30°C, Surface As Received

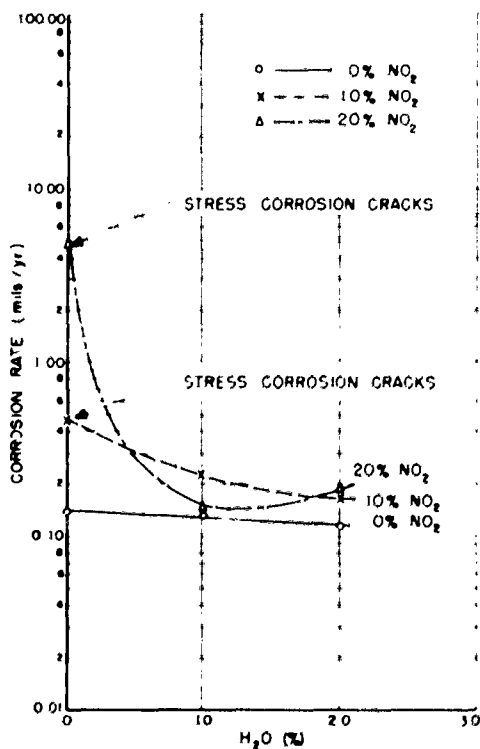


Figure 2. Average Corrosion Rates of Commercially Pure Titanium in FNA at 30°C, Surface Sandblasted

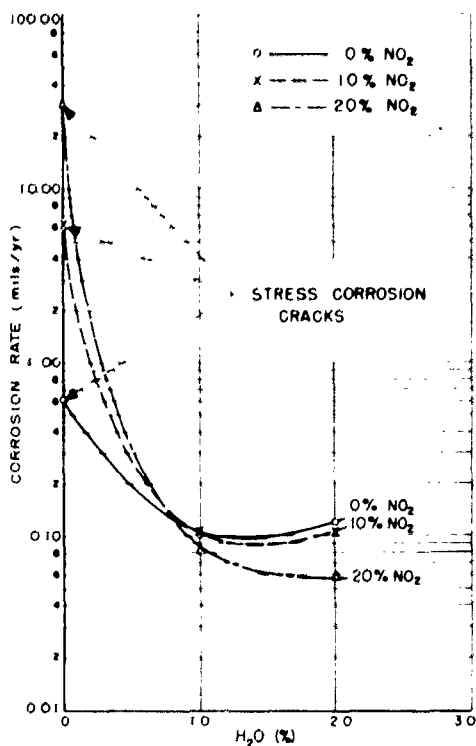


Figure 3. Average Corrosion Rates of Ti - 8% Mn Alloy in FNA at 30°C, Surface As Received

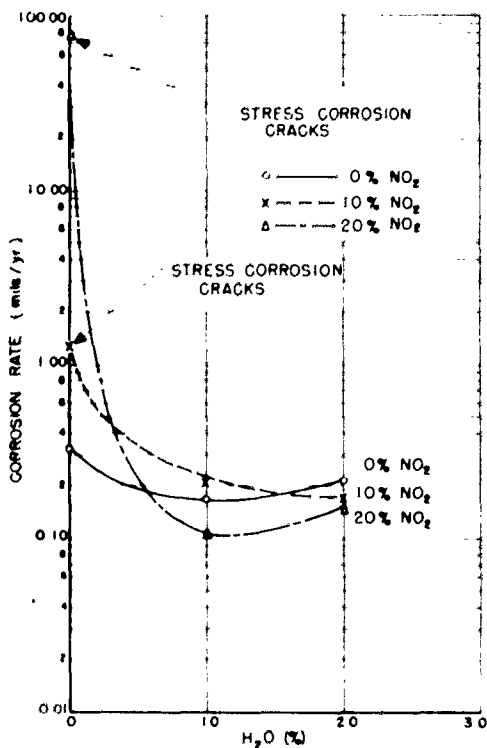


Figure 4. Average Corrosion Rates of Ti - 8% Mn Alloy in FNA at 30°C, Surface Sandblasted



Figure 5. Photomicrograph of Longitudinal Section of Commercially Pure Titanium Sheet (250X)



Figure 6. Photomicrograph of Transverse Section of Commercially Pure Titanium Sheet with 263 Hours Prior Exposure to 20%  $\text{NO}_2$  Anhydrous FNA (250X)



Figure 7. Photomicrograph of Longitudinal Section of Ti - 8% Mn Alloy (250X)



Figure 8. Photomicrograph of Transverse Section of Ti - 8% Mn Alloy with 48 Hours Prior Exposure to 20% NO<sub>2</sub> Anhydrous FNA (150X)





Figure 9  
Photomicrograph of  
Longitudinal-Edge  
Section of a Por-  
tion of the Sam-  
ple of Figure  
8, Unetched  
(250X)

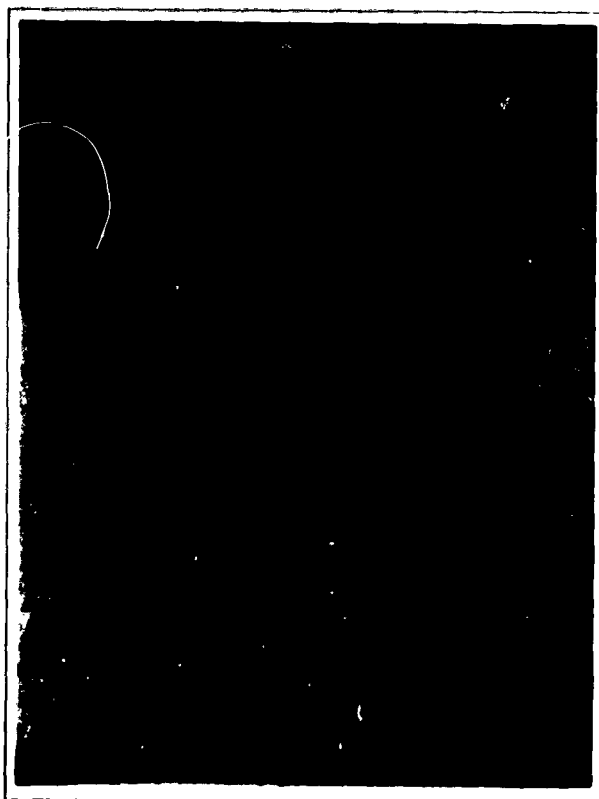


Figure 10  
Photomicrograph of Corner of Ti -  
8% Mn Sheet. Sample Heated in  
Vacuum  $\frac{1}{2}$  Hour at 788°C,  
Quenched While in Vac-  
uum into Liquid Nitro-  
gen. Exposed to 20%  
NO<sub>2</sub> Anhydrous  
FNA for 24  
Hours, Un-  
etched  
(250X)



Figure 11. Photomicrograph of Base of Crack  
in Sample Shown in Figure 10, Etched (250X)



Figure 12. Photomicrograph of Transverse Section of Ti - 8% Mn Alloy  
with Treatment Similar to Figure 10, Oblique Illumination,  
Etched (250X)



Figure 13  
Same Section As Fig-  
ure 12 but with Pol-  
arized Light

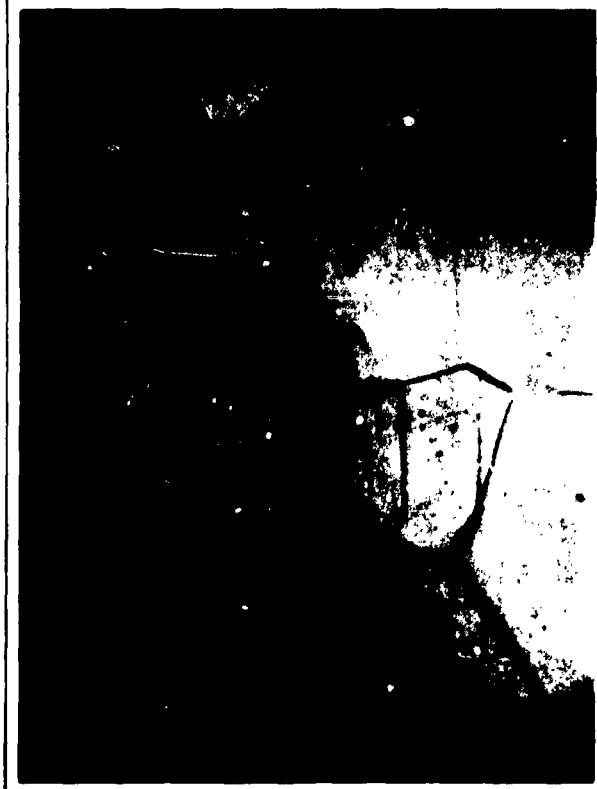


Figure 14  
Photomicrograph of Ti - 8% Mn  
Heated *in vacuo* to 788°C,  
Quenched into Ice Water,  
All-Beta Phase, Etched  
(250X)

## REFERENCES

1. *Metals Handbook*. Cleveland: The American Society for Metals, 1948.
2. Evans, U. R., *Metallic Corrosion Passivity and Protection*. London: Edward Arnold and Company, 1948.
3. *Symposium on Stress-Corrosion Cracking of Metals*. York (Pa.): American Society for Testing Materials, 1945.
4. Uhlig, H. H., *Corrosion Handbook*. New York: John Wiley and Sons, 1948.
5. *Corrosion*. New York: The International Nickel Co. Inc., 1951.
6. Rittenhouse, J. B., Vango, S. P., and Mason, D. M., *Corrosion and Ignition of Titanium Alloys in Fuming Nitric Acid. I. Study of Some Chemical and Metallurgical Factors*, Progress Report No. 26-1. Pasadena: Jet Propulsion Laboratory, September 30, 1955.
7. Mason, D. M., Taylor, L. L., and Keller, H. F., *Storability of Fuming Nitric Acid*, Report No. 20-72. Pasadena: Jet Propulsion Laboratory, December 28, 1953.
8. Runnells, O. J. C., and Pidgeon, L. M., "Observations on the Preparation of Iodine Titanium," *Transactions of the American Institute of Mining and Metallurgical Engineers*, 194: 843-847, 1952.
9. Robertson, G. D., Mason, D. M., and Sage, B. H., *Electrolytic Conductance of the Ternary System of Nitric Acid--Nitrogen Dioxide--Water at 32°F and Atmospheric Pressure*, Progress Report No. 20-155. Pasadena: Jet Propulsion Laboratory, November 12, 1951.
10. *X-Ray Diffraction Data Cards*. Philadelphia: American Society for Testing Materials, 1950.
11. Cadoff, I., and Palty, A. E., *Binary Alloys of Titanium with Carbon, Nitrogen, Oxygen and Boron*, Final Report. New York: Engineering Research Division, New York University, October 31, 1954.
12. Craighead, C. M., Leuning, G. A., and Jaffee, R. I., "Nature of Line Markings in Titanium and Alpha Titanium Alloys," *Transactions of the American Institute of Mining and Metallurgical Engineers*, 194: 1317-1319, 1952.
13. Kroll, W. J., "Commercial Titanium and Zirconium," *Journal of the Franklin Institute*, 260 (No. 3): 169-192, September, 1955.
14. Larsen, R. P., Shor, R. S., Feder, H. M., and Flikkema, D. S., *A Study of the Explosive Properties of Uranium-Zirconium Alloys*, ANL No. 5135. Lemont (Ill.): Argonne National Laboratory, July, 1954.

## REFERENCES (Cont'd)

15. Adelman, B. R., *An Apparatus for the Determination of the Impact Sensitivity of Explosive Compounds*, Memorandum No. 20-66, Pasadena: Jet Propulsion Laboratory, May 28, 1951.
16. *Rem-Cru Titanium Manual*. Midland (Pa.): Rem-Cru Titanium, Inc., 1954.
17. Maykuth, D. J., Ogden, H. R., and Jaffee, R. L., "Titanium-Manganese System," *Transactions of the American Institute of Mining and Metallurgical Engineers*, 197: 225-230, 1953.
18. Finlay, W. L., and Vordahl, M. B., "The Titanium Alloys Today," *Metals Progress*, 61 (No. 2): 173-178, February, 1952.
19. Samans, C. H., *Engineering Metals and Their Alloys*. New York: The MacMillan Company, 1949.
20. *Republic Titanium and Titanium Alloys*. Mansillon (Ohio): Republic Steel Corp., 1954.

INITIAL DISTRIBUTION  
Contract AF 33(616)-3066

- |   |   |
|---|---|
| 1. Naval Ordnance Test Station<br>Inyokern, China Lake, California<br>Attn: Mr. R. W. Sprague                               | 10. Titanium Metal Corp.<br>Henderson, Nevada<br>Attn: Mr. S. A. Herren   |
| 2. U. S. Naval Air Rocket Test Station<br>Lake Nemi<br>Dover, New Jersey<br>Attn: Mr. Terlizzo-Propellant Division          | 11. Mallory Sharon Titanium Corp.<br>Niles, Ohio<br>Attn: Mr. Lee Bunch   |
| 3. Aerojet General Corporation<br>Azusa, California<br>Attn: Mr. C. Ross  | 12. North American Aviation Inc.<br>Downey, California<br>Attn: Mr. J. C. Berrer, Director  |
| 4. Boeing Aircraft Corporation<br>Box 3107<br>Seattle 14, Washington<br>Attn: Mr. R. H. Nelson, Project Engineer<br>MX-1559 | 13. Reaction Motors, Inc.<br>Rockaway, New Jersey<br>Attn: Mr. W. P. Munger, Chief Engr.  |
| 5. Boeing Aircraft Corporation<br>Box 3107<br>Seattle 14, Washington<br>Attn: Process Group                                 | 14. Battelle Memorial Institute<br>Columbus, Ohio<br>Attn: Mr. C. B. Voldrich   |
| 6. Bell Aircraft Corporation<br>Niagara Falls, New York<br>Attn: Mr. H. A. Campbell   | 15. Battelle Memorial Institute<br>Columbus, Ohio<br>Attn: Liquid Propellant Handbook Group   |
| 7. United States Dept. of Interior<br>Bureau of Mines<br>Washington 25, D. C.<br>Attn: Mr. T. H. Miller, Acting Director    | 16. Commanding General<br>Redstone Arsenal<br>Huntsville, Alabama<br>Attn: Technical Library  |
| 8. Rem-Cru Titanium Inc.<br>Midland, Pa.<br>Attn: Mr. W. L. Finley  | 17. Allegheny Ludlum Corp.<br>Water Villiet, New York<br>Attn: W. Dyrkacz   |
| 9. Republic Steel Corp.<br>Mansillon, Ohio<br>Attn: Mr. V. Whitmore   | 18-35. Commander<br>Wright Air Development Center<br>Air Research and Development Command<br>Wright-Patterson Air Force Base, Ohio<br>Attn: WCRTH-3 |